ELSEVIER

International Journal of Mass Spectrometry 193 (1999) 57–68

International Journal of Mass Spectrometry

Proton-bound cluster ions in ion mobility spectrometry

Robert G. Ewing[a,1], Gary A. Eiceman[a,*], J.A. Stone[b]

[a]*Department of Chemistry and Biochemistry, New Mexico State University, Las Cruces, NM 88003, USA*
[b]*Department of Chemistry, Queen's University, Kingston, Ontario K7L 3N6, Canada*

Received 29 January 1999; accepted 13 July 1999

Abstract

Gaseous oxygen and nitrogen bases, both singly and as binary mixtures, have been introduced into ion mobility spectrometers to study the appearance of protonated molecules, and proton-bound dimers and trimers. At ambient temperature it was possible to simultaneously observe, following the introduction of molecule A, comparable intensities of peaks ascribable to the reactant ion $(H_2O)_nH^+$, the protonated molecule AH^+ and $AH^+ \cdot H_2O$, and the symmetrical proton bound dimer A_2H^+. Mass spectral identification confirmed the identifications and also showed that the majority of the protonated molecules were hydrated and that the proton-bound dimers were hydrated to a much lesser extent. No significant peaks ascribable to proton-bound trimers were obtained no matter how high the sample concentration. Binary mixtures containing molecules A and B, in some cases gave not only the peaks unique to the individual compounds but also peaks due to asymmetrical proton bound dimers AHB^+. Such ions were always present in the spectra of mixtures of oxygen bases but were not observed for several mixtures of oxygen and nitrogen bases. The dimers, which were not observable, notable for their low hydrogen bond strengths, must have decomposed in their passage from the ion source to the detector, i.e. in a time less than ~5 ms. When the temperature was lowered to −20 °C, trimers, both homogeneous and mixed, were observed with mixtures of alcohols. The importance of hydrogen bond energy, and hence operating temperature, in determining the degree of solvation of the ions that will be observed in an ion mobility spectrometer is stressed. The possibility is discussed that a displacement reaction involving ambient water plays a role in the dissociation. (Int J Mass Spectrom 193 (1999) 57–68) © 1999 Elsevier Science B.V.

Keywords: Proton-bound dimer; Ion mobility spectrometry; Asymmetric

1. Introduction

Ion mobility spectrometers are used to detect trace amounts of gaseous materials. Since they operate at atmospheric pressure they have seen much use e.g. in monitoring atmospheres for trace pollutants, in detecting traces of narcotics and explosives which are desorbed from particulate matter and in battlefields to detect war gases [1,2]. In all the above mentioned situations, the ideal instrument response is the generation of a single ion that is unique to the particular compound of interest. Problems in spectral interpretation may arise when more than one ion is detected and the spectral pattern becomes complex. The origins of such problems may be due to a multicomponent sample yielding ions with similar mobilities that lead to several peaks in the spectrum which may be nonresolvable, an overload of sample which results in ion solvation and broadened and overlapping peaks, or a combination of both. Since water vapor is always

* Corresponding author. E-mail: geiceman@nmsu.edu
[1] Permanent address: Idaho National Engineering and Environmental Laboratory, Idaho Fall, ID 83415-2208.

PII S1387-3806(99)00141-4

present in a mobility spectrometer, hydration of the ions of interest is always possible and the ions detected may or may not be hydrated. The degree of hydration of an ion will depend not only on the concentration of water vapor but also on the temperature and the nature of the ion. In general, ions undergo dehydration reactions at a high temperature and in a low moisture atmosphere. Also, ions where the charge is delocalized hydrate to a lesser extent than do charge-localized ions under the same conditions [3]. Both the hydrated and the nonhydrated forms of the same ion will be linked by reactions as they travel through the drift region and will constitute a single peak in the mobility spectrum.

At high concentrations of analyte, so-called dimer and trimer ions may be formed. For example, a molecule A, which is to be detected as a protonated ion, may be present in the ion source as AH^+ at low concentrations of A but with increasing concentration the proton-bound dimer, A_2H^+, and the proton-bound trimer, A_3H^+, may also be present. Whether or not all these ions reach the detector will depend on their stabilities under the conditions of instrument operation. Much data is present in the literature on the interaction between ions and molecules that are pertinent to the interpretation of mobility spectra [4–15]. Tabulations of pertinent thermodynamic data on clustering reactions have been compiled [16].

The formation of proton-bound dimers and trimers of a substantial number of oxygen and nitrogen bases in the drift tube of a mobility spectrometer at ambient pressure is described in this article. The influence of temperature and sample concentration has been studied and the results are interpreted in terms of available thermodynamic information and of the operational characteristics of the mobility spectrometer.

2. Experimental

Two mobility spectrometers used in this study were modified versions of the military-grade analyzer, the Chemical Agent Monitor (Graseby Ionics Ltd., Watford, Herts., UK). The permeation source for acetone was removed in order for the reagent ion in all

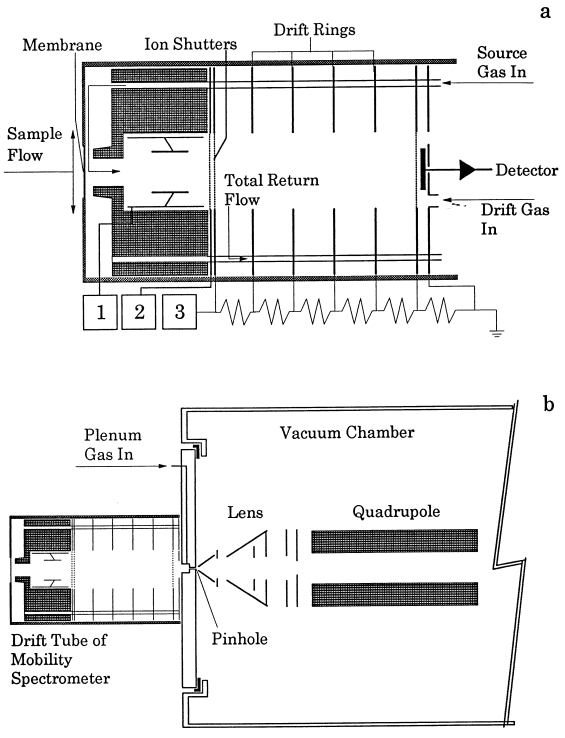

Fig. 1. Schematic diagram of (a) the ion mobility spectrometer and (b) the mobility spectrometer-mass spectrometer. Labels 1, 2, and 3 are, respectively, the high voltage supplies for the ion source, the shutter, and the drift tube.

experiments to be the hydrated proton. A schematic diagram of the drift tube of this mobility spectrometer is shown in Fig. 1(a). The ionization region contains 10 mCi of ^{63}Ni. The drift region between shutter and ion collector is 3.6 cm long and has an electric field strength of 244 V/cm. The shutter pulse width is 180 μs with a repetition rate of 40 Hz. The inlet sample flow is isolated from the ionization region by a semipermeable methyl silicone membrane, 10–15 μm thick, which assists in maintaining stable moisture levels in the drift and ionization regions. There are no temperature readouts for the device; the inlet nozzle is at ~40 °C, the membrane is at ~100 °C to facilitate sample permeation and the gas in the drift region is approximately at ambient temperature. Signals were processed using digital signal averaging (usually 100–1000 scans per spectrum) with a commercial interface board and supporting software (Advanced Signal Processor, Graseby Ionics, Ltd.).

A second mobility spectrometer was interfaced to a triple quadrupole mass spectrometer (TAGA 6000, SCIEX, Inc., Toronto, Ontario, Canada) as shown also in Fig. 1(b) and was used for the identification of ions in separate experiments. The drift tube was virtually identical to that described previously except that it had no membrane at the inlet and the detector end was modified slightly for mounting on the interface flange of the mass spectrometer. The detector plate of the drift tube was replaced with a Teflon® gas-tight adapter, so that ions were sampled into the lens assembly of the mass spectrometer through a pinhole membrane on the vacuum flange of the TAGA 6000. The last conducting ring in the drift region of the ion mobility spectrometry (IMS) was placed at +1400 V and the interface plate was at +650 V. As with the stand-alone IMS instruments, the drift gas flow was unidirectional, entering at the Teflon® adapter. A small flow of clean nitrogen gas (the plenum flow) passed over the pinhole of the mass spectrometer and then entered the drift region of the mobility spectrometer. In the operation of the mobility spectrometer/mass spectrometer, the ion shutter of the mobility spectrometer was always fully open to provide a maximum ion yield and gave only total ion composition without correlation to specific mobilities. The operating parameters of the mass spectrometer for the identification of ions and for collision-assisted dissociation (CAD) studies were routine values [17], except that the potential difference between the pinhole and the first lens was kept at the minimal value of 1 V in order to minimize collisionally assisted decomposition of ions in this region. Fifty scans were averaged to obtain a mass spectrum.

The sample presented to the mobility spectrometer was generated as follows. Air was bubbled at less than 1 mL/min into a reservoir of a neat, liquid chemical contained in a 1 mL glass vessel. The air was delivered to and removed from the vessel by using 20–50 cm lengths of 0.05 mm i.d. (inner diameter) fused-silica capillary tubing. If mixtures were to be created, an identical system was placed in parallel to the first and the flows from both were combined in a short section of 3 mm o.d. (outer diameter) glass tubing. The vapor-saturated air was supplemented with a flow of 10–120 mL/min of clean air and the resulting stream was split using a Swagelock "T" union (El Paso Valve and Fitting Co., El Paso, TX) so that one part was vented and the other (5–100 mL/min as required) was directed into another dilution chamber. A supplemental flow of 300–1200 mL/min of air was used for a final dilution. All flows were adjusted using Nupro fine metering valves (El Paso Valve and Fitting, Co., El Paso, TX). The bottled air was scrubbed using activated charcoal and 13× molecular sieve and its moisture content was maintained at about 10 ppm.

Suitable sample concentrations were obtained by adjusting the split flow ratio as well as the dilution flows for both stages in the vapor generator. The sample flow was directed through a container that accepted the nozzle of the ion mobility spectrometer. The flow was not restricted, the excess being allowed to vent around the nozzle. Adjustments were made until a suitable mobility spectrum was obtained. Once set, the intensities of the ions were monitored for 10–15 minutes to assure the stability of the delivered sample concentration before mobility spectra were collected.

The chemicals used were obtained from laboratory holdings and from various manufacturers. All were analytical or reagent grade and were used as received after the identities and purities were confirmed by gas chromatography/mass spectrometry assays.

3. Results

When an IMS is operated at ambient temperature in the positive ion mode in the absence of sample and with air as both the drift gas and the sample carrier gas, the major reactant ion peak (RIP) observed has been identified as due to ions of general formula $(H_2O)_nH^+$ [18]. The formation of the reactant ions from the initial ionization of the air by the ^{63}Ni β particles involves a complex sequence of ion/molecule reactions and the value of n is dependent on the moisture level and temperature of the system. If equilibrium is established quickly in the ionization region and holds throughout the drift region then it

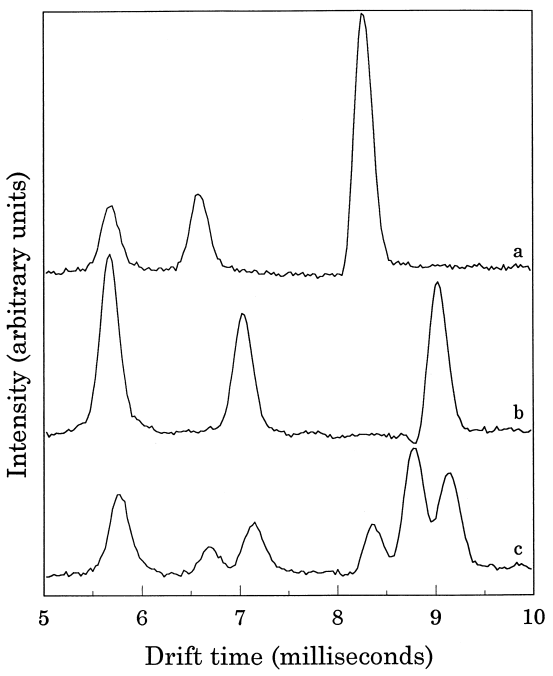

Fig. 2. Mobility spectrum of (a) cyclohexanone, (b) 4-heptanone, and (c) a mixture of the two obtained at ambient temperature.

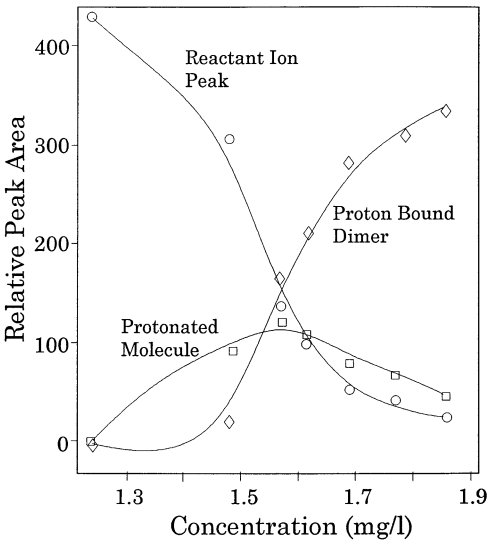

Fig. 3. Relative abundances of the reagent ion, protonated 2-butanone and its proton-bound dimer as functions of concentration in the mobility spectrum of 2-butanone obtained at ambient temperature.

can be calculated from thermodynamic data [19,20] that the most probable value of *n* in the presence of 10 ppm moisture, is 4. When molecules of a compound capable of accepting protons from the reagent ions are introduced to the ionization region via the semipermeable membrane, the RIP decreases as protons are transferred. Simultaneously a second peak appears, usually at a greater drift time than the RIP, representing an ion with lesser mobility than the reactant ion. With increasing amounts of sample, the RIP decreases further, the new peak grows and peaks representing ions with even lower mobility may appear.

Typical mobility spectra for compounds introduced singly into the source are shown in Fig. 2(a) and (b) for cyclohexanone and 4-heptanone, respectively. Identification of the peaks with the mobility spectrometer/mass spectrometer showed the first peak to appear was due to a mixture of the protonated molecule AH^+ and its monohydrate, $AH^+ \cdot H_2O$. This mobility peak will henceforth be referred to as the protonated molecule peak. The second peak was ascribed to the nonhydrated proton-bound dimer A_2H^+, with a small contribution from $A_2H^+ \cdot H_2O$. The relationship between the areas of the RIP and the two new peaks and the sample concentration, in this case for 2-butanone, is shown in Fig. 3. It is seen that as the RIP decreases, the protonated molecule peak at first increases in area, attains a maximum yield, and then decreases as the intensity of the proton-bound dimer increases. It is to be noted that under the experimental conditions, the reactant ions, the protonated molecule and the proton-bound dimer can all appear at the detector with approximately the same intensities when the sample is in a certain concentration range. The equal intensities in Fig. 3 are around 1.55 μg/L in the case of 2-butanone.

When two sample streams were combined, all the previously observed peaks for the two compounds introduced separately were still present, and a new one might or might not appear. This new peak was situated between the two proton-bound dimer peaks of the pure components. In Fig. 2(c), the new peak appears at a drift time of 8.8 ms, almost exactly midway between the two proton-bound dimer peaks

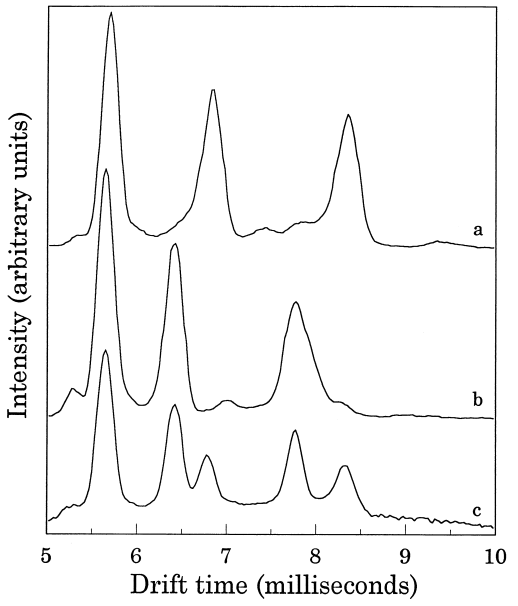

Fig. 4. Mobility spectrum for (a) *n*-butylamine, (b) *n*-propyl ether, and (c) a mixture of the two at ambient temperature.

of the two compounds, 4-heptanone and cyclohexanone. The mass spectrum of the mixture also showed a peak, *m/z* 213, which was not present in the mass spectrum of either of the compounds alone. The CAD spectrum of this ion showed two major product ions, *m/z* 115 and *m/z* 99 that correspond to protonated 4-heptanone and protonated cyclohexanone, respectively. The new peak in the mobility spectrum of the mixture is therefore due to the asymmetrical proton-bound dimer containing the two ketones. It was found that it was not always possible to produce such a peak with some mixed vapor streams. Such an example is illustrated by Fig. 4 that shows the mobility spectra for (a) *n*-butylamine alone, (b) di-*n*-propyl ether alone, and (c) a mixture of the two. The sample concentrations and their relative values were varied over as wide a range as possible, but no asymmetric proton-bound dimer peak was observed.

The results for a series of mixtures are presented in Table 1. In the table, columns three and four show the drift times, relative to those of the RIP, of the proton-bound dimers of the individual components and column five shows the values for the asymmetric dimers that are observed. The absence of a value signifies that no such dimer could be produced under any circumstances at ambient temperature.

Protonated monomers and proton bound dimers were observed when the drift tube was operated at ambient temperature and attempts were unsuccessful in creating a proton-bound trimer through increases in sample vapor concentrations. In fact, no significant peaks were observed with drift times higher than those of the proton-bound dimers, whether for single compounds or for mixtures. However, peaks did appear in the mobility spectra of some compounds when the drift tube was cooled to subambient temperatures and these were identified by mass spectrometry as proton-bound trimers. In the example shown in Fig. 5(a) for 2-propanol at −20 °C, four peaks are present. An increase of sample concentration did not lead to any increase in this number of peaks but did increase the intensities of the later peaks at the expense of the earlier ones. The mass spectrum in Fig. 5(b) allows identification of the peaks as due to the RIP (*m/z* 37, 55, and 73), the protonated molecule and its mono- and dihydrate (*m/z* 61, 79, and 97), the proton-bound dimer and its monohydrate (*m/z* 121 and 139), and the proton-bound trimer (*m/z* 181). No ions with more than three 2-propanol molecules solvating the proton were observable at −20 °C.

When a mixed vapor stream entered the IMS at −20 °C, both symmetrical and asymmetrical proton-bound dimers and trimers were observed. The example shown in Fig. 6(a) is the mobility spectrum of a mixture of 2-propanol and 2-butanol. The large number of peaks and the relatively narrow spread in drift times has resulted in severe overlap of the peaks. The use of a deconvolution procedure [21] shows the presence of ten significant peaks in the spectrum which are also shown in Fig. 6(a). The mass spectrum of the same system, although with a different concentration ratio of the alcohols, shown in Fig. 6(b), allows identification of the IMS peaks. The protonated molecular hydrates are at *m/z* 79 (2-propanol) and *m/z* 93 (2-butanol); the proton-bound dimers are at *m/z* 121 $(2\text{-propanol})_2$, *m/z* 135 (2-propanol/2-butanol), and at *m/z* 149 $(2\text{-butanol})_2$; the proton-bound trimers are at

Table 1
Normalized drift times for symmetrical (A_2H^+ and B_2H^+) and asymmetrical (AHB^+) proton-bound dimers and calculated half-lives of asymmetrical proton-bound dimers

A	B	A_2H^+	B_2H^+	AHB^+	$-\Delta H^{0}$ [b] (kcal mol^{-1})	k_{-7} [c] (s^{-1})	$t_{1/2}$ [d] (s)
t-Butanol	1-Pentanol	1.34	1.54	1.43	29.5	4.3*E* − 05	1.6*E* + 04
Propyl ether	Butyl acetate	1.46	1.62	1.54	29.4	5.1*E* − 05	1.4*E* + 04
2-Propanol	1-Pentanol	1.25	1.54	1.39	29.3	6.0*E* − 05	1.1*E* + 04
Cyclohexanone	4-Heptanone	1.46	1.59	1.53	29.2	7.2*E* − 05	9.7*E* + 03
Propylacetate	2-Butanone	1.49	1.26	1.37	28.9	1.2*E* − 04	5.8*E* + 03
2-Propanol	t-Butanol	1.25	1.34	1.29	28.9	1.2*E* − 04	5.8*E* + 03
2-Butanone	Propyl ether	1.24	1.46	1.35	28.8	1.4*E* − 04	4.9*E* + 03
Butanone	Cyclohexanone	1.24	1.46	1.36	28.6	2.0*E* − 04	3.5*E* + 03
Acetone	2-Butanone	1.12	1.24	1.17	28.5	2.3*E* − 04	3.0*E* + 03
Butanone	4-Heptanone	1.24	1.59	1.43	28.3	3.3*E* − 04	2.1*E* + 03
2-Propanol	2-Butanol	1.25	1.35	1.30	28.1	4.6*E* − 04	1.5*E* + 03
2-Butanol	Butyl acetate	1.36	1.62	1.47	28.1	4.6*E* − 04	1.5*E* + 03
2-Butanol	Propyl ether	1.35	1.48	1.39	28.0	5.4*E* − 04	1.3*E* + 03
2-Butanol	1-Pentanol	1.35	1.54	1.45	27.8	7.6*E* − 04	9.1*E* + 02
Cyclohexanone	2-Butanol	1.46	1.35	1.38	27.8	7.6*E* − 04	9.1*E* + 02
Acetone	Cyclohexanone	1.12	1.46	1.28	27.6	1.1*E* − 03	6.5*E* + 02
4-Heptanone	2-Butanol	1.59	1.35	1.46	27.6	1.1*E* − 03	6.5*E* + 02
Acetone	4-Heptanone	1.12	1.59	1.35	27.3	1.8*E* − 03	3.9*E* + 02
1-Butanol	2-Butanone	1.40	1.26	1.32	27.0	2.9*E* − 03	2.4*E* + 02
Cyclohexanone	t-Butanol	1.46	1.34	1.39	27.0	2.9*E* − 03	2.4*E* + 02
Pentanoic acid	Butyl acetate	1.44	1.62	1.54	26.9	3.5*E* − 03	2.0*E* + 02
4-Heptanone	t-Butanol	1.59	1.34	1.46	26.7	4.8*E* − 03	1.4*E* + 02
Cyclohexanone	2-Propanol	1.46	1.25	1.33	26.4	8.0*E* − 03	8.6*E* + 01
4-Heptanone	2-Propanol	1.59	1.25	1.40	26.1	1.3*E* − 02	5.2*E* + 01
n-Butylamine	Propyl ether	1.38	1.47	···[e]	25.1	7.2*E* − 02	9.6*E* + 00
n-Butylamine	Propylacetate	1.38	1.48	···	25.1	7.2*E* − 02	9.6*E* + 00
n-Butylamine	Butyl acetate	1.38	1.62	1.53	25.1	7.2*E* − 02	9.6*E* + 00
n-Butylamine	2-Butanone	1.38	1.26	1.35	24.5	2.0*E* − 01	3.5*E* + 00
DMMP	2-Butanone	1.46	1.26	1.36	24.1	3.9*E* − 01	1.8*E* + 00
2,4-Lutidine	Butyl acetate	1.47	1.62	···	22.6	4.9*E* + 00	1.4*E* − 01
2-Butanone	2,4-lutidine	1.26	1.49	···	22.0	1.3*E* + 01	5.2*E* − 02
DMMP	1-Butanol	1.46	1.40	···	21.6	2.6*E* + 01	2.6*E* − 02
2,4-Lutidine	2-Butanol	1.48	1.35	···	21.3	4.4*E* + 01	1.6*E* − 02
2,4-Lutidine	Butylamine	1.48	1.38	···	20.8	1.0*E* + 02	6.8*E* − 03
n-Butylamine	2,4-lutidine	1.39	1.49	···	20.8	1.0*E* + 02	6.8*E* − 03
2,4-Lutidine	1-Butanol	1.49	1.41	···	19.7	6.5*E* + 02	1.1*E* − 03

[a] Drift times normalized to that of the reagent ion.
[b] Calculated enthalpy change for the formation of the hydrogen bond in AHB^+.
[c] Rate constant for the dissociation of AHB^+, calculated using Eq. (7) with a temperature of 298 K.
[d] Half-life of AHB^+.
[e] ··· indicates not observed.

m/z 181 (2-propanol)$_3$, *m/z* 195 ((2-propanol)$_2$/2-butanol), *m/z* 209 (2-propanol/(2-butanol)$_2$), and *m/z* 223 (2-butanol)$_3$. There are also small peaks in the mass spectrum representing the nonhydrated proton-bound molecules and the proton-bound dimers.

4. Discussion

Proton transfer to sample molecules from the reactant hydrated proton formed all ions in this study. The rate at which such proton transfer reactions occur

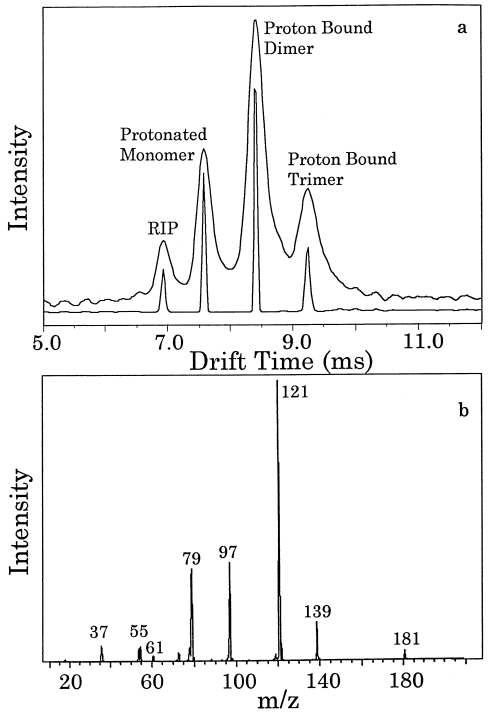

Fig. 5. Mobility spectrum and (a) deconvoluted mobility spectrum and (b) mass spectrum for 2-propanol obtained at −20 °C.

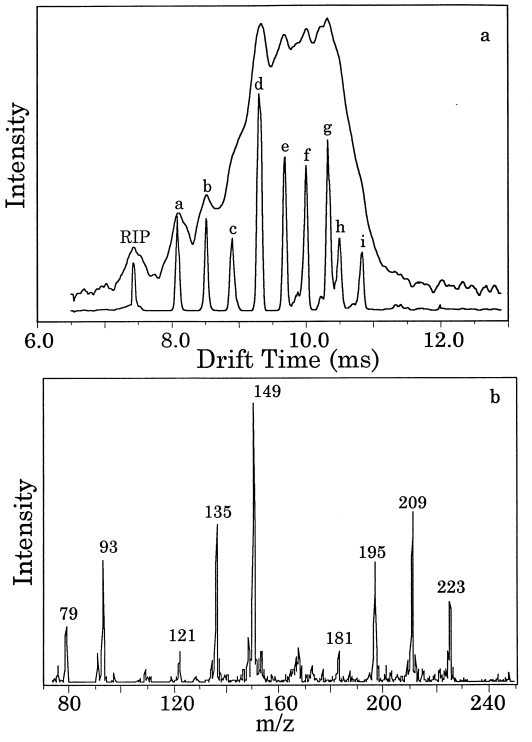

Fig. 6. Mobility spectrum (upper curve) and (a) deconvoluted spectrum (lower curve) and (b) mass spectrum, for a mixture of 2-propanol and *n*-butanol at −20 °C. In the upper part, the mobility peaks are designated as: a and b, the protonated molecules; c, d, and e, the proton bound dimers; f, g, h, and i, the proton bound trimers.

in an atmospheric pressure chemical ionization source has been discussed in terms of the efficiencies of the reactions as functions of temperature [3,9]. The discussion is directly applicable to the situation in an IMS. It can be calculated, using experimentally determined thermodynamic data, that if equilibrium is attained in the ionization region, held at 25 °C, in the presence of 10 ppm water, the major reactant ion will be $(H_2O)_4H^+$ [19,20]. The effective proton affinity of four water molecules is the proton affinity of water plus the energy of hydration of H_3O^+ by three water molecules. The value is 233 kcal/mol. Proton transfer can occur with high efficiency to another molecule if the basicity of the molecule is higher than that collectively of four water molecules, or if the resulting protonated molecule is readily solvated by water in the proton transfer reaction. None of the bases used in this work have a proton affinity higher than 233 kcal/mol (Table 2) but all can be hydrated in a proton transfer process [3] and the proton transfer reaction is expected to occur as shown in

$$H_3O^+(H_2O)_n + A \Rightarrow AH^+(H_2O)_m + (n - m + 1)H_2O \quad (1)$$

The presence of the monohydrates of the protonated oxygen bases in the mass spectra is consistent with the transfer of solvation water in the proton transfer process to these bases, which have much lower proton affinities than the nitrogen bases. However, unlike high pressure mass spectrometry or atmospheric pressure mass spectrometry, the ions which are created in the ion source of the mobility spectrometer are drawn through the drift region containing purified gas. In traversing the drift region, each ion suffers $\sim 10^8$ collisions with neutral mole-

Table 2
Proton affinity values[a]

Compound	Proton affinity[b]
2,4-Lutidine	230.1
n-Butylamine	220.2
DMMP[c]	217.8[d]
4-Heptanone	202.0
Cyclohexanone	201.0
Propyl ether	200.3
Propyl acetate	200.0
Butyl acetate	200.0[e]
2-Butanone	197.7
2-Butanol	194.8
Acetone	194.0
t-Butanol	191.8
4-Pentanoic acid	190.5[f]
2-Propanol	189.5
1-Butanol	188.6
1-Pentanol	188.6[g]

[a]Data from [30], unless otherwise stated.
[b]Units kcal mol^{-1}.
[c]Dimethyl methylphosphonate.
[d]From [33].
[e]Taken as equal to the value for *n*-propyl acetate.
[f]Taken as equal to the value for propanoic acid.
[g]Taken as equal to the value for *n*-butanol.

cules of which $\sim 10^3$ collisions will be with water molecules, present at 10 ppm. Any hydrated ions formed in the proton transfer reaction will change their initial identities as they attain equilibrium with the water in the drift gas before being sampled into the mass spectrometer. The relative concentrations of ions in equilibrium with the drift gas can be calculated when the requisite thermodynamic information is available. For example, the computed relative abundances of the protonated molecule and its null, first, second, third, and fourth hydrates, respectively, are: for acetone—10^{-5}, 0.48, 0.38, 0.12, and 0.02 [22] and for dimethyl ether—10^{-6}, 1, 0.24, 0.08, and 0.002 [23]. The corresponding values for *n*-propylamine are 0.04, 1, 0.063, 10^{-4}, and 10^{-7}, respectively [5]. Neither *n*-propylamine nor dimethyl ether were used in this study but the values calculated may be taken as being representative for the amines and ethers employed. The relative abundances of the symmetrical proton-bound dimer of acetone and its first three hydrates are calculated from available thermodynamic data to be 0.99, 0.0047, 6×10^{-5}, and 10^{-6} [22].

The mass spectra show much less hydration of the ions than predicted by the above calculations, but do show qualitative agreement in that the protonated oxygen bases are much more highly hydrated than the proton-bound dimers and the protonated amines. The transfer of ions, with impressed forward momentum, through the plenum gas and the pressure gradient of the IMS/MS interface can change the degree of ion hydration by collisional dissociation. This obviously has occurred, and the observed mass spectra therefore give no quantitative information regarding the extent of hydration of the ions in the drift tube. Each mobility peak contains an ion and its hydrates, and the mass spectra can be used to identify the core ion but cannot give information regarding the distribution of the ions amongst the bare and hydrated forms.

4.1. Proton bound dimers in ion mobility spectrometry

In all experiments, sufficient sample was present to form one or more proton-bound dimers. With a mixture of two bases, A and B, the dimers A_2H^+, B_2H^+, and ABH^+ would be formed in the source region of the IMS. These ions would tend toward being in equilibrium with the neutral molecules A and B. The possible reactions are exemplified by

$$AH^+ + A \Leftrightarrow A_2H^+ \quad (2)$$

$$BH^+ + B \Leftrightarrow B_2H^+ \quad (3)$$

$$AH^+ + B \Leftrightarrow ABH^+ \quad (4)$$

$$BH^+ + A \Leftrightarrow ABH^+ \quad (5)$$

but they may be more complex if the protonated molecules become hydrated, the proton-bound dimers may also be formed in exothermic displacement reactions, as illustrated by

$$AH^+H_2O + A \Leftrightarrow A_2H^+ + H_2O \quad (6)$$

After the ions enter the drift region, where ideally no neutral molecules, other than those of the drift gas are present, only the reverse of these reactions can occur and all the proton-bound dimers will commence

to dissociate. These reactions removing the dimers may be either first order dissociations at the high pressure limit, or second order displacement reactions, exemplified by the reverse of Eq. (6).

Table 1 shows the drift times, relative to that of the RIP, of all the proton-bound dimers, both symmetrical and asymmetrical, which were observed at ambient temperature. Mixtures of any of the oxygen bases—alcohols, ketones, ethers, carboxylic acids, and esters, fed into the ionization region, lead to the formation of asymmetrical dimers. The relative drift times of the asymmetrical dimers are seen to always have values between the times for the two symmetrical dimers, and in many cases are very close to the arithmetic mean of the two values. This implies that in most cases the collision cross section between an asymmetrical dimer ion and the drift gas molecules is simply, as expected if the cross section is mainly due to geometric considerations, the sum of the cross sections of the individual components.

Nine of the mixtures listed at the bottom of Table 1 did not yield discernible peaks ascribable to asymmetrical dimer ions, even though the symmetrical dimers were readily obtained. This could of course be due to the fact that in each of these systems the sought-for peak was coincident with one of the symmetrical dimer peaks. There is no reason to expect that this would be the case and, in support of this contention, the "missing ions" were not present in the mass spectra. Therefore, for these mixtures, either the asymmetrical dimer was never formed or, if it was formed, it dissociated before reaching the detector plate. The former should not be the case since asymmetrical dimer ions from similar amine and oxygen bases have been obtained in high pressure mass spectrometric studies and thermodynamic data for their formation have been obtained [7]. If the asymmetrical dimers were formed but dissociation was complete during transit, then the half-lives of their dissociation reactions must be less than a few milliseconds. The decomposition of a proton-bound dimer could occur either in a first order reaction, the reverse of Eqs. (2)–(5), or in a displacement reaction with water, the only suitable molecule in the drift gas. A rough estimate of the lifetime of a proton-bound dimer may be made from available thermodynamic data as described below.

The association of a protonated molecule AH^+ with a neutral molecule B

$$AH^+ + B + M \Rightarrow ABH^+ + M \tag{7}$$

is actually a third order process and hence the reaction rate can be dependent on total pressure.

Such third order behavior has been shown, e.g. in high pressure mass spectrometric studies of the kinetics of hydration of H_3O^+ at elevated temperatures and total pressures of a few Torr [19,24]. In a high pressure mass spectrometric study carried out at ~1 Torr, the rate constants for the formation of each of $CH_3NH_3^+ \cdot CH_3NH_2$ and $(CH_3)_2NH_3^+ \cdot (CH_3)_2NH_2$ attained pressure independent values in the temperature range 210–364 K that were not too different from the collision rate constants [25]. The limiting rate constants were within a factor of 5 of the computed collision rate constants. It follows that at the high pressure and ambient temperature of the present IMS study, it is to be expected that most of the reactions leading to proton-bound dimer formation and dissociation are at the high-pressure limit, with rate constants equal to the collision rate constants and independent of total pressure. By the principle of microscopic reversibility, the dissociation reactions for these proton-bound dimers should also be independent of pressure and can be treated as pseudo-first-order reactions. In this case, a proton-bound dimer with a lifetime less than its potential IMS drift time (~10 ms) would have pseudo-first-order rate constant for dissociation somewhat greater than the reciprocal of the lifetime, i.e. $\sim 10^2$/s. The rate constants for dissociation, k_{7-} may be estimated, by using

$$K_7 = e^{-\Delta G^0/RT} = e^{-\Delta H^0/RT} e^{\Delta S^0/RT} = (k_{7+}/k_{7-})\, P^0 \tag{8}$$

where K_7 is the equilibrium constant for reaction (7), k_{7+} is the forward rate constant, and P^0 is the standard pressure of one atmosphere. At the high-pressure limit, k_{7+} is assumed equal to the collision rate constant, which may be readily calculated [26].

The standard free energy changes for the formation

of the proton-bound dimers of the molecules examined in this study have not been measured, but their approximate values may be obtained from estimations of the standard enthalpy and entropy changes. The standard enthalpy changes for the formation of both symmetrical and asymmetrical dimers have not been measured for most of the compounds in Table 1. However, the standard enthalpies of association of symmetrical $–OH^+ \cdots O–$ dimers is constant at 32 ± 1.5 kcal/mol [27] and the standard enthalpies of formation of symmetrical $–NH^+ \cdots N–$ dimers is constant at 23 ± 1.5 kcal/mol [7,28,29]. A linear correlation between the standard enthalpies of binding and the differences in proton affinities for the participants in asymmetrical $–NH^+ \cdots O–$ dimers allows estimations of the hydrogen bond energies and a limited number of nitrogen base pairs provide data for asymmetrical $–NH^+ \cdots N–$ hydrogen bonds [7]. A linear correlation between the differences in proton affinity of oxygen bases, XO, and water and the $–XOH^+ \cdots OH_2$ bond enthalpies serves as a basis for computing the hydrogen bond energies of the asymmetrical proton-bound dimers of the oxygen bases. Adjustment of the proton affinity values to a later evaluated scale [30] leads to the following parameters (a in kcal/mol, b dimensionless) for the linear correlations, $\Delta H^0 = a - b \times \Delta PA$: $–NH^+ \cdots O–$, (30.1 ± 0.6, 0.25 ± 0.01), $–OH^+ \cdots O–$; (29.5 ± 0.6, 0.27 ± 0.02); $–NH^+ \cdots N–$; (23.0 ± 1.0, 0.22 ± 0.06). It is to be noted that the correlation for the $–OH^+ \cdots O–$ hydrogen bond leads to the slightly lower value of 29.5 ± 0.6 kcal/mol for symmetrical dimers than the 32 ± 1.5 kcal/mol of Larson and McMahon [27]. The estimated enthalpy changes for the formation of the hydrogen bonds of the asymmetrical dimers are presented in column 6 of Table 1. Measured entropy changes for hydrogen bond formation are usually in the range 20–30 cal/K mol [16] with the values for base pairs similar to those at the bottom of Table 1 generally at the upper end of the range [7]. A fixed entropy change for hydrogen bond formation of −30 cal/K mol was used to calculate $\Delta G°$ and hence obtain the rate constants, k_{-7}, shown in column 7 of Table 1, for the dissociation of the asymmetrical proton-bound dimers. The half-lives of the dimers, derived from these first order rate constants according to Eq. (8), are given in column eight of Table 1.

Since a constant ΔS^0 value has been used in the calculation of the half-lives, any differences in the values of the half-lives between different proton-bound dimers depend solely on the calculated hydrogen bond energies. As expected, the proton-bound asymmetrical dimers, which are observed are those that have the largest hydrogen bond energies, namely those containing two oxygen bases. All but one of these pairs have calculated hydrogen bond energies greater than 25 kcal/mol. There is a large uncertainty in these bond energies of at least ±2 kcal/mol. By contrast, all except two of the asymmetrical dimers which are not observed in the mobility spectra of mixtures have computed hydrogen bond energies less than 25 kcal/mol, and the exceptions have computed bond strengths of 25.1 kcal/mol. If the ambient temperature of the drift gas is taken to be 298 K, the calculated half-lives at 298 K of the asymmetrical proton-bound dimers, shown in column eight of Table 1, range from 10^4 to 10^{-3} s. All the "nonappearing" dimers have small half-lives, although many of the values are greater than the expected drift times for nondissociating ions. The computed half-lives are only approximations because of uncertainties in the thermodynamic data used in their computation and the fact that the ambient temperature is unknown. The closed systems of the IMS instruments did not allow monitoring of drift tube gas temperature. The ambient temperature was probably greater than the supposed 298 K and hence all the computed half-lives for decomposition are upper estimates.

A low hydrogen-bond strength is obviously a factor that determines whether or not a proton-bound dimer has a long enough lifetime to reach the detector. However, the hydrogen bond strength cannot be the only factor for the nonappearance of an asymmetrical dimer since the hydrogen bond strengths of proton-bound symmetrical dimers containing two nitrogen bases also have hydrogen bond energies less than 25 kcal/mol [7,28,29] and are present in the mobility spectra (Fig. 3). A second contribution to the instability might be that in addition to a low hydrogen

bond energy, the entropy of activation for the dissociation of these asymmetrical dimers is more favorable, but again it is difficult to see why, in this respect, these particular dissociations are favored relative to others. A third contribution, which should be more important for the asymmetrical dimers containing both an oxygen and a nitrogen base, is that one or more water molecules present in the drift gas take part in a displacement reaction

$$AH^+B + nH_2O \Rightarrow AH^+\cdot(H_2O)_n + B \quad (9)$$

This would be a multistep process if more than one water molecule were required before dissociation occurred. If displacement by a single molecule is possible, the reaction involves the replacement of one hydrogen bond by another. The replacement of a $–NH^+ \cdots O–$ bond by a $–OH^+ \cdots OH_2$ bond can be close to thermoneutral. For example, the measured hydrogen bond energy of the hydrate of protonated di-*n*-propyl ether is 21.3 kcal/mol [7] so that with a $–NH^+ \cdots O–$ hydrogen bond energy between protonated *n*-butylamine and di-*n*-propyl ether, the displacement reaction of Eq. (9) is endothermic by only ~3 kcal/mol. This value is much less than the 21.3 kcal mol^{-1} for the non-water-assisted decomposition

$$n\text{-}C_4H_9NH_3^+ \cdots O(n\text{-}C_3H_7)_2 + H_2O \Rightarrow n\text{-}C_4H_9NH_2 + (n\text{-}C_3H_7)_2OH^+ \cdots OH_2 \quad (10)$$

The proton would remain with the protonated base having the highest hydration energy and this would in general be the oxygen base since nitrogen bases, having the higher proton affinities, have significantly lower hydration energies than oxygen bases.

4.2. Proton bound trimers of alcohols at −20 °C

When the temperature of the IMS is lowered below ambient, then further solvation of protonated molecules by both water and other neutral molecules present in the ionization region is possible. In addition, the decreased temperature will prolong the lifetimes of the solvated ions, such as proton-bound dimers and trimers, in their passage through the drift region where solvating molecules, other than water, are absent. This is exemplified by the mobility spectra for *n*-propanol obtained at −20 °C shown in Fig. 5(a). The mass spectrum in Fig. 5(b) shows the presence of the proton-bound trimer, which was not observable at ambient temperature, the monohydrate of both the protonated molecule and the proton-bound dimer, and the dihydrate of the protonated molecule.

The deconvolution of the mobility spectrum in Fig. 6(a) and the mass spectrum in Fig. 6(b) for a mixture of *n*-propanol and *n*-butanol, shows that all possible combinations of molecules are present in the proton-bound dimers and trimers. There is evidence in the mass spectrum of small peaks due to monohydrates of the two most intense proton-bound dimer ions. As noted earlier, neither the relative heights of the deconvoluted peaks of the mobility spectrum nor the peak heights in the mass spectrum should be taken as showing the actual ionic distribution in the IMS. The designation of the peaks is confirmed by the plots (not shown) of relative drift times, obtained from the deconvoluted mobility spectrum, versus the masses of the nonhydrated ions. There is a linear correlation between the masses of the ions and the drift times for each of the series of ions, proton-bound molecules (admittedly only two points), dimers and trimers. The slopes of the lines increase with increasing number of solvating alcohol molecules, signifying as expected, a decreasing contribution to the collision cross section for each additional molecule bound to the proton. If the degree of hydration of the ions were known and could be taken into consideration, then all points would shift horizontally with increase of ionic mass, the points for the more highly hydrated protonated molecules moving the greatest distances. However, the degree of solvation of ions within each group is expected to be very similar so that the slopes of the correlation lines would still distinguish the three ion types.

The enthalpy of binding to the proton of successive alcohol molecules in clusters decreases monotonically. For example, the enthalpies for the addition of the second, third, and fourth methanol molecules to $CH_3OH_2^+$ are reported by Grimsrud and Kebarle [31] to be 33.1, 26.3, and 16.1 kcal/mol and by Meot-Ner

[32] as 32.1, 21.0, and 16.1 kcal/mol. Solvation by a weakly bound fourth alcohol molecule was not observable even at −20 °C, presumably because such highly solvated ions had lifetimes, with respect to loss of the fourth and higher molecules, shorter than the transit time through the drift tube.

5. Conclusions

It has been shown that even though high concentrations of neutral molecules are fed into the ionization region of an ion mobility spectrometer, whether or not proton-bound dimer ions are observed depends on the types of molecules constituting the dimers as well as on the temperature of operation. Symmetric proton-bound dimers were found under ambient conditions for all molecules studied: alcohols, ketones, ethers, aliphatic amines, and aromatic amines. Proton-bound asymmetric dimers were observed for all pairs of oxygen bases, but were not observed for some nitrogen/oxygen and nitrogen/nitrogen base pairs. The pairs for which proton-bound dimers were not observed are characterized by weak hydrogen bonds, computed to be below 24 kcal/mol. Although these dimers will be formed by association of protonated and neutral molecules in the ionization region, their lifetimes with respect to decomposition are shorter than the transit time from shutter to collector. The reason for this cannot be simply low hydrogen bond strength since symmetric dimers with comparable bond strengths are observed. Favorable entropies of activation for decomposition and the participation of water in displacement reactions are presented as possibilities. A lowering of the temperature increases the lifetimes, and hence allows the detection, of proton-bound trimer ions, both symmetric and asymmetric, which were not observable under ambient conditions.

Acknowledgements

The financial support from NASA (grant no. NAGY-4558) and US Army Research Office (grant no. DAAH04-95-1-0541) is gratefully acknowledged. Caroline Tapphorn is thanked for technical assistance.

References

[1] G.A. Eiceman, Z. Karpas, Ion Mobility Spectrometry, CRC, Boca Raton, FL, 1994.
[2] Plasma Chromatography, T.W. Carr (Ed.), Plenum, New York, 1984.
[3] J. Sunner, M.G. Ikonomou, P. Kebarle, Anal. Chem. 60 (1988) 1308.
[4] M. Meot-Ner, J. Am. Chem. Soc. 105 (1983) 4906.
[5] M. Meot-Ner, J. Am. Chem. Soc. 106 (1984) 1265.
[6] M. Meot-Ner, J. Am. Chem. Soc. 106 (1984) 278.
[7] M. Meot-Ner, J. Am. Chem. Soc. 106 (1984) 1257.
[8] M. Meot-Ner, J. Am. Chem. Soc. 114 (1992) 3312.
[9] J. Sunner, G. Nicol, P. Kebarle, Anal. Chem. 60 (1988) 1300.
[10] M. Meot-Ner, L.W. Sieck, S. Scheiner, X. Duan, J. Am. Chem. Soc. 116 (1994) 7848.
[11] K. Hiraoka, S. Fujimaki, K. Aruga, S. Yamabe, J. Phys. Chem. 98 (1994) 8295.
[12] W.Y. Feng, M. Goldenberg, C. Lifshitz, J. Am. Soc. Mass. Spectrom. 5 (1994) 695.
[13] K. Hiraoka, Bull. Chem. Soc. Jpn. 60 (1987) 2555.
[14] J.S. Klassen, A.T. Blades, P. Kebarle, J. Phys. Chem. 99 (1995) 15509.
[15] P. Kebarle, J. Mass Spectrom. 32 (1997) 922.
[16] R.G. Keesee, A.W. Castleman, J. Phys. Chem. Ref. Data 15 (1986) 1011.
[17] Z. Karpas, G.A. Eiceman, C.S. Harden, R.G. Ewing, P.B.W. Smith, Org. Mass Spectrom. 29 (1994) 159.
[18] S.H. Kim, K.R. Betty, F.W. Karasek, Anal. Chem. 50 (1978) 2006.
[19] A.J. Cunningham, J.D. Payzant, P. Kebarle, J. Am. Chem. Soc. 97 (1972) 7627.
[20] P. Kebarle, S.K. Searles, A. Zolla, J. Scarborough, M. Arshadi, J. Am. Chem. Soc. 89 (1967) 6393.
[21] S.E. Bell, R.G. Ewing, Y.F. Wang, G.A. Eiceman, Analyt. Chim. Acta. 303 (1995) 163.
[22] M. Meot-Ner, S. Scheiner, W.O. Yu, J. Am. Chem. Soc. 120 (1998) 6980.
[23] K. Hiraoka, E.P. Grimsrud, P. Kebarle, J. Am. Chem. Soc. 96 (1974) 3359.
[24] M. Meot-Ner, F.H. Field, J. Am. Chem. Soc. 99 (1977) 998.
[25] M. Meot-Ner, F.H. Field, J. Am. Chem. Soc. 97 (1975) 5339.
[26] T. Su, J. Chem. Phys. 100 (1994) 4703.
[27] J.W. Larson, T.B. McMahon, J. Am. Chem. Soc. 104 (1982) 6255.
[28] R. Yamdagni, P. Kebarle, J. Am. Chem. Soc. 95 (1973) 3504.
[29] M. Meot-Ner, L.W. Sieck, J. Am. Chem. Soc. 105 (1983) 2956.
[30] E.P.L. Hunter, S.G. Lias, J. Phys. Chem. Ref. Data 27 (1998) 413.
[31] E.P. Grimsrud, P. Kebarle, J. Am. Chem. Soc. 95 (1973) 7939.
[32] M. Meot-Ner, J. Am. Chem. Soc. 108 (1986) 6189.
[33] J.A. Stone, unpublished results.